Amino Acids (2012) 43:2431–2441
DOI 10.1007/s00726-012-1322-y

ORIGINAL ARTICLE

Improvement of enzymatic stability and intestinal permeability of deuterohemin-peptide conjugates by specific multi-site N-methylation

Qing-Guang Dong · Yong Zhang · Meng-Shu Wang · Jiao Feng · Hai-Hong Zhang · Yong-Ge Wu · Tie-Jun Gu · Xiang-Hui Yu · Chun-Lai Jiang · Yan Chen · Wei Li · Wei Kong

Received: 16 March 2012 / Accepted: 8 May 2012 / Published online: 7 June 2012

Abstract The deuterohemin-peptide conjugate, DhHP-6 (Dh-β-AHTVEK-NH_2), is a microperoxidase mimetic, which has demonstrated substantial benefits in vivo as a scavenger of reactive oxygen species (ROS). In this study, specific multi-site N-methylated derivatives of DhHP-6 were designed and synthesized to improve metabolic stability and intestinal absorption, which are important factors for oral delivery of therapeutic peptides and proteins. The DhHP-6 derivatives were tested for (1) scavenging potential of hydrogen peroxide (H_2O_2); (2) permeability across Caco-2 cell monolayers and everted gut sacs; and (3) enzymatic stability in serum and intestinal homogenate. The results indicated that the activities of the DhHP-6 derivatives were not influenced by N-methylation, and that tri-N-methylation of DhHP-6 could significantly increase intestinal flux, resulting in a two- to threefold higher apparent permeability coefficient. In addition, molecules with N-methylation at selected sites (e.g., Glu residue) showed high resistance against proteolytic degradation in both diluted serum and intestinal preparation, with 50- to 140-fold higher half-life values. These findings suggest that the DhHP-6 derivatives with appropriate N-methylation could retain activity levels equivalent to that of the parent peptide, while showing enhanced intestinal permeability and stability against enzymatic degradation. The tri-*N*-methylated peptide Dh-β-AH(Me)T(Me)V(Me)EK-NH_2 derived from this study may be developed as a promising candidate for oral administration.

Keywords DhHP-6 · ROS · *N*-methylated peptide · Permeability · Enzymatic stability

Abbreviations

ROS	Reactive oxygen species
APx	Ascorbate peroxidase
PEG	Polyethylene glycol
DMF	*N*,*N*-dimethylformamide
HOBT	1-Hydroxy-1H-benzotriazole
NMM	*N*-methylmorpholine
HATU	O-(7-azabenzotriazol-1-yl)-*N*,*N*,*N*′,*N*′-tetramethyluronium hexafluorophosphate
HOAt	3H-[1,2,3]-triazolo[4,5-b]pyridin-3-ol
DIEA	*N*,*N*-diisopropylethylamine
NMP	*N*-methylpyrrolidone
PyBop	Benzotriazole-1-yl-oxytripyrrolidino-phosphonium hexafluorophosphate
TFA	Trifluoroacetic acid
R-CHCA	R-cyano-4-hydroxycinnamic acid
DMEM	Dulbecco's Modified Eagle's Medium
TEER	Transepithelial electrical resistance
HBSS	Hank's balanced salt solution

Q.-G. Dong and Y. Zhang contributed equally to this work.

Electronic supplementary material The online version of this article (doi:10.1007/s00726-012-1322-y) contains supplementary material, which is available to authorized users.

Q.-G. Dong · Y. Zhang · M.-S. Wang · J. Feng · H.-H. Zhang · Y.-G. Wu · T.-J. Gu · X.-H. Yu · C.-L. Jiang · Y. Chen (✉) · W. Li · W. Kong (✉)
National Engineering Laboratory for AIDS Vaccine, College of Life Science, Jilin University, Qianjin Street 2699, Changchun 130012, Jilin, People's Republic of China
e-mail: chen_yan@jlu.edu.cn

W. Kong
e-mail: weikong@jlu.edu.cn

Introduction

Oxybiotic organisms generate reactive oxygen species (ROS) by the partial reduction of molecular oxygen yielding superoxide anions, hydrogen peroxide (H_2O_2) and hydroxyl radicals. Excessive ROS are presumed to induce cellular damage by oxidative modification of cellular biomacromolecules (such as lipids, proteins and nucleic acid) that leads to cell and tissue dysfunction (Reed 2011; Berlett and Stadtman 1997; Nakabeppu et al. 2007). Antioxidant treatment has long been considered an efficient therapy for a wide variety of disorders, in which oxidative stress is believed to play a significant role (Rice-Evans and Diplock 1993; Day 2004). A novel deuterohemin-linked 6-mer peptide conjugate, DhHP-6 (Dh-β-AHTVEK-NH_2), belonging to a metalloporphyrin class of therapeutic catalytic antioxidants, was successfully synthesized in our laboratory. Its structural design was based on the lead compounds of ascorbate peroxidase (APx) and microperoxidase (MP-9), resulting from digestion of cytochrome C with proteolytic enzymes. The heme vinyl group was reduced to prevent oxidation, while addition of the 6-mer peptide AHTVEK to the DhHP-6 molecule, as a relatively conserved sequence in MP and APx, improved its water-solubility and electron transfer activity (Wang et al. 2004). Compared to MP, DhHP-6 has desirable properties, including simple preparation and improved chemical stability. DhHP-6 has been demonstrated to improve cell survival and prevent apoptosis, which would be relevant in potential treatments of cardiovascular disease, cataracts, diabetes and aging (Wang et al. 2004; Guan et al. 2010).

Oral administration is considered the most convenient method for drug delivery. However, the development of orally available peptides, either by improving their intestinal transport and/or by enhancing their stability against enzymatic degradation, has become a significant challenge in the past decade (Lee 2002; Mahato et al. 2003; Hamman et al. 2005). Strategies for increasing peptide enzymatic stability and improving intestinal absorption include cyclization, substitution by non-natural amino acids, covalent attachment of polyethylene glycol (PEG) or lipidation (Nestor 2009; Gentilucci et al. 2010). However, N-methylation has obvious advantages over these other methods. *N*-methylated peptides have been shown to improve pharmacological characteristics, such as lipophilicity, conformation constraint and proteolytic stability, and to enhance binding affinity and receptor subtype selectivity (Linde et al. 2008; Ovadia et al. 2011; Chatterjee et al. 2008).

In this study, a series of compounds derived from DhHP-6 with specific multi-site *N*-methyl modifications were designed and synthesized with the aim of improving resistance to protease degradation and enhancing intestinal permeability, which are considered two important factors for oral delivery of therapeutic peptides. After measuring their activity, the stability of these compounds in mouse serum and intestinal homogenate, as well as permeability through Caco-2 cell monolayers and everted gut sacs was evaluated. In addition, the degradation pathways of DhHP-6 and its N-methylated derivatives mediated by hydrolytic enzymes were deduced based on analysis of their fragments by reversed-phase high-performance liquid chromatography (RP-HPLC) and matrix-assisted laser desorption ionization/time of flight mass spectra (MALDI–TOF-MS). Our results showed that tri-*N*-methylated DhHP-6 exhibited excellent proteolytic stability and increased permeability without activity loss, suggesting that specific multi-site N-methylation can be a feasible strategy for the development of orally administered DhHP-6.

Materials and methods

Chemicals

The following were purchased from GL Biochem Shanghai Ltd. (Shanghai, China): N-Fmoc protected amino acids, including Fmoc-Lys(Boc)-OH, Fmoc-Glu(OtBu)-OH, Fmoc-Val-OH, Fmoc-Thr(tBu)-OH, Fmoc-His(Trt)-OH, Fmoc-β-Ala-OH, Fmoc-N-Me-Glu(OtBu)-OH, Fmoc-N-Me-Val-OH and Fmoc-N-Me-Thr(tBu)-OH; rink amide resin and solvents for peptide synthesis, including *N*,*N*-dimethylformamide (DMF), piperidine, 1-hydroxy-1H-benzotriazole (HOBT), *N*-methylmorpholine (NMM), o-(7-azabenzotriazol-1-yl)-*N*,*N*,*N*′,*N*′-tetramethyluronium hexafluorophosphate (HATU), 3H-[1,2,3]-triazolo[4,5-b] pyridin-3-ol (HOAt), *N*,*N*-diisopropylethylamine (DIEA), *N*-methylpyrrolidone (NMP), benzotriazole-1-yl-oxytripyrrolidinophosphonium hexafluorophosphate (PyBop), trifluoroacetic acid (TFA), methylphenyl ether, phenol, methanol and ether. Other reagents and solvents were of analytical grade and obtained commercially.

Peptide synthesis

When small amounts of peptide are needed, such as screening for desired peptides, the simplest strategy is to use *N*-methylated amino acids directly as building blocks (Chatterjee et al. 2008). Deuterohemin was prepared following an optimized procedure (Liu et al. 2001), and peptide chains were synthesized using a standard N-Fmoc/tBu solid-phase peptide synthesis protocol (Lister-James et al. 2001). Rink amide methylbenzhydrylamine (MBHA) resin (0.75 g, 0.33 mmol/g) was pre-swollen in DMF for 15 min and washed with DMF (6 × 1 min). The Fmoc

deprotection step was carried out with 20 % piperidine in DMF (15 min), followed by washing with DMF (6 × 1 min). The coupling reaction was conducted until Kaiser ninhydrin (reaction with primary amine) and chloranil tests (reaction with secondary amine) became negative. The unmodified amino acids were introduced by adding Fmoc-amino acids (4 equiv), PyBop (4 equiv), HOBT (4 equiv), NMM (6 equiv) and deprotected resin in DMF (5 ml) with shaking for 1 h at room temperature, followed by washing with DMF (6 × 1 min). The N-Me-amino acids were coupled by mixing deprotected resin, Fmoc-N-Me-amino acids (6 equiv), HATU (6 equiv), HOAt (4 equiv) and DIEA (12 equiv) in NMP (5 ml) with shaking for 4 h at room temperature (2×). The resin was then washed with NMP and DMF (3 × 1 min). These steps (removal of Fmoc group and coupling of Fmoc-amino acid) were repeated until all amino acids in the peptide sequence were coupled. Coupling of deuterohemin to the peptide chain was carried out by mixing Dh (3 equiv), PyBop (3 equiv) and NMM (12 equiv) in NMP (5 ml) for 1 h at room temperature. Next, the resin was washed with NMP (5 × 1 min), DMF (3 × 1 min) and methanol (3 × 1 min) and dried under vacuum. Peptide cleavage from the resin and removal of side chain protecting groups were carried out with a pre-cooled mixture of 92.5 % TFA, 2.5 % methylphenyl ether, 2.5 % phenol and 2.5 % water for 1 h. The cleaved peptide solution was dropped into cold ether, and the precipitate was washed with ether.

RP-HPLC

The crude product was centrifuged and purified by RP-HPLC (Agilent, USA) using a YMC ODS-A semi-preparative column (250 × 20 mm, 10 μm YMC Co., Ltd. Japan). Linear gradient elution (0 min 10 % B; 120 min 60 % B) with eluent A (0.1 % TFA in water) and eluent B (0.1 % TFA in acetonitrile) was used at a flow rate of 20 ml/min. Peaks were detected at 386 nm. Fractions containing the peptide were collected and lyophilized. Purities of all synthesized peptides were determined by analytical RP-HPLC, and molecular weights and peptide sequences were confirmed by MALDI–TOF-MS/MS.

The analytical HPLC apparatus was equipped with a quaternary pump, auto-sampler and diode array detector (Agilent 1200, USA). The chromatographic separation was performed on an Eclipse XDB C_{18} column (5 μm, 4.6 × 150 mm, Agilent). Mobile phase A consisted of 10 % acetonitrile in water (0.1 % TFA), and mobile phase B consisted of 90 % acetonitrile in water (0.1 % TFA). Samples were eluted with a linear gradient from 10 % B to 20 % B within 5 min; 20 % B to 32 % B within 12 min, and 32 % B to 52 % B within 2 min, and then changed back to 10 % B for re-equilibration for 10 min. Other parameters were: flow rate, 1.0 ml/min; column temperature, 25 °C; injection volume, 20 μl; detected wavelength, 386 nm.

MS

The MS analyte (0.5 μl) was combined with the matrix [0.5 μl, 50 mM R-cyano-4-hydroxycinnamic acid (R-CHCA) in 70 % acetonitrile and 0.1 % TFA], and then 1 μl of this mixture was spotted onto a stainless steel MALDI target plate to dry at room temperature. The target plate was loaded into a MALDI–TOF–TOF 5800 mass spectrometer (AB SCIEX, USA) equipped with a neodymium: yttrium–aluminum–garnet laser in reflection positive-ion mode (laser wavelength 349 nm, laser intensity 2,000–2,500, focus 1200). Data were accumulated between 500 and 4,000 *m/z*.

Lipophilicity

The 1-octanol/water partition coefficient (log $P_{o/w}$) was determined by the shake-flask method (Takács-Novák et al. 1994). 1-Octanol and water were presaturated prior to the experiment. The vials were shaken overnight in a water bath shaker (ZHWY-110X50, Shanghai, China). Both phases (1-octanol and water) were analyzed by RP-HPLC. The final log $P_{o/w}$ value was calculated by dividing the concentration (C) of the compound in the two phases (partition coefficients $= C_{1-\text{octanol}}/C_{\text{water}}$).

Peroxidase activity

Peroxidase activity was measured by monitoring the H_2O_2-dependent oxidation of ascorbate spectrophotometrically (Mandelman et al. 1998). The reaction mixtures consisted of potassium phosphate (50 mM, pH 7.4), disodium edetate (EDTA-Na_2, 0.1 mM), ascorbate (0.5 mM), H_2O_2 (0.3 mM) and 2 μM DhHP-6 derivatives or MP-11 (a control enzyme, Sigma) in a total volume of 3 ml. Assays were conducted at ambient temperature (25 °C). The reaction was initiated by adding the sample, and the decrease in the absorbance at 290 nm was recorded 60 s after this addition (NanoDrop 2000, Thermo, USA). Activity was determined by dividing the ΔAbs by $\varepsilon = 2.8\ \text{mM}^{-1}\ \text{cm}^{-1}$. One unit of activity is defined as 1 μmol ascorbate oxidized in 1 min. Specific activity was calculated by dividing the units of activity by μmol of DhHP-6 derivatives used in the assay.

Determination of in vitro stability

Blood was collected from the mouse vena caudalis and placed at 37 °C for 2 h to extrude serum. The serum was

separated by centrifugation (Eppendorf 5424, Germany) at 3,000 rpm for 10 min. The intestinal segment between the duodenum and the ileum was isolated from the killed mouse. After washing in ice-cold saline (50 ml), the intestinal tissue was cut into small pieces and placed in 5 ml of pH 7.5 phosphate-buffered solution (PBS) for processing in a tissue homogenizer in an ice bath (200 rpm, 2 min). The homogenate was centrifuged at 10,000 rpm for 10 min, and the supernatant was collected (Han et al. 1998). The total protein concentration in the supernatant was measured by ultraviolet spectroscopy at 280 nm. Homogenates were diluted to 10 mg protein/ml as necessary. Serum and intestinal homogenate were stored at −80 °C until further analysis.

The serum and intestinal tissue homogenate samples (100 µl) were combined with DhHP-6 derivatives (100 µl) at final concentrations of 0.1 mM and 0.5 mM, respectively. The analytes were then incubated at 37 °C. To follow the kinetics of proteolysis of the DhHP-6 derivatives, the incubation was terminated at specified time points by adding 200 µl of TFA (12 %) and mixed by vortexing for 60 s. The precipitated proteins were separated by centrifugation (10,000 rpm, 5 min). The clear supernatant was adjusted with equivalent sodium hydroxide (1 M) to pH 6.0–7.0 and then analyzed by HPLC.

The proteolysis kinetics of DhHP-6 and its derivatives were analyzed by following the decrease in the concentration of the intact peptide as a function of time. First-order rate kinetics were acquired, described by the equation $y = be^{-kt}$ (nonlinear regression via Origin version 6.0), and the half-lives of DhHP-6 and the derivatives were calculated as $t_{1/2} = \ln 2/k$, where y is the normalized concentration (%) of the residual intact peptide at time t; b, the initial peptide concentration; k, the first-order rate constant; and t, the incubation time in hours (Grunwald et al. 2009). The appropriate fractions were collected for identification of the chromatographic peaks by MALDI–TOF-MS analysis.

In vitro permeability study

Caco-2 cells were obtained from the Cell Bank of the Chinese Academy of Sciences (Shanghai, China). The cells were maintained in Dulbecco's Modified Eagle's Medium (DMEM), supplemented with 10 % fetal bovine serum, 1 % nonessential amino acids and 2 mM L-glutamine (GIBCO Invitrogen, Germany), and grown at 37 °C in 5 % CO_2 atmosphere with relative humidity of 95 %. Cells in the passage range of 60–66 were seeded at a density of 2.5×10^5 cells/cm^2 on polycarbonate membrane culture inserts (0.4 µm pore size and 0.6 cm^2 surface area) in 24-transwell plates (12 mm) (Millipore, USA). The culture medium was changed every other day, and transport studies were performed 21–23 days after seeding when the cells were fully differentiated and the transepithelial electrical resistance (TEER) value of the Caco-2 cell monolayer measured in each transwell using a Millicel-ERS meter (Millipore) was stable (500–800 Ω cm^2). The media from both sides of the monolayers were removed, and the cells were washed with Hank's balanced salt solution (HBSS) (400 µl) and incubated for 30 min at 37 °C. The buffers were removed and replaced with 400 µl of HBSS on the basolateral side as well as 200-µl sample solution (1 mM dissolved in HBSS and sterile filtered through 0.22-µm membranes) on the apical side of the monolayer in each transwell. After the cells were incubated at 37 °C for 120 min, samples were taken from the basolateral side to conduct HPLC analysis (Gao et al. 2001). To compare the transport rate of fluorescein and DhHP-6 derivatives without the functional barrier of epithelial tight junctions, an EDTA-Na_2 solution (1 mM) was prepared using D-HBBS (without Ca^{2+}/Mg^{2+}) to open the tight junctions. The solution was applied to the Caco-2 cell monolayers for 10 min at 37 °C. The solution was then removed, and the cells were washed three times with D-HBBS. Test samples were added to Caco-2 cells as described above.

Freshly isolated gut sacs of rat ileum were washed with iced Ring solution. The gut sacs (approximately, 4 cm each) were carefully everted with a glass rod, filled with oxygenated tissue culture medium (0.4 ml DMEM) at 37 °C and the ends were ligated with silk. Each gut sac was then placed in a tube containing 5 ml of pre-gassed (95 % O_2; 5 % CO_2) DMEM (containing 1 mM sample) at 37 °C. The use of tissue culture medium ensures excellent tissue viability and metabolic activity and is a considerable improvement on the basic technique (Barthe et al. 1998). The gut sacs were incubated at 37 °C in a water bath (100 cycles/min). After 60 min, gut sacs were removed, washed in 0.9 % NaCl solution and blotted dry. The serosal fluid was drained into small tubes following centrifugation at 12,000 rpm for 5 min, and the supernatant was analyzed by HPLC.

The apparent permeability coefficient (P_{app}) for each compound was calculated using the equation, $P_{app} = 1/(C_0 \times A) \times dQ/dt$, where dQ/dt is the steady state rate of appearance of the drug on the receiver side, C_0 is the initial concentration of the drug on the donor side, and A is the exposed tissue surface area (2 cm^2 for tissues and 0.6 cm^2 for Caco-2 cells).

Statistical analysis

Results were evaluated using Student's t test (SPSS version 3.0) for independent data, and differences were considered significant when $P < 0.05$.

Results and discussion

Peptide synthesis

Catalytic antioxidants (macrocyclics, salens and metalloporphyrins) have generally been considered a radical approach to ROS therapeutics (Day 2004). For example, M40403 (macrocyclic) shows protective effects in myocardial ischemia and reperfusion injury, and EUK134 (salen) reduces renal dysfunction and injury caused by oxidative and nitrosative stress, while AEOL10150 (metalloporphyrin) inhibits tobacco smoke-induced lung inflammation (Masini et al. 2002; Smith et al. 2002; Chatterjee et al. 2004). In this study, N-methylated derivatives of the iron porphyrin analog DhHP-6 were synthesized with the aim of developing a drug with greater oral availability. We have also considered whether the amide linkage needs to be N-methylated before the peptides were designed. However, the N-methylation design of the peptides was simplified to attain our objective, since we gained information on the stability of DhHP-6 through preliminary experiments as well as the N-methylation effects on conformation of the peptide through the following reference (Chatterjee et al. 2008). Therefore, Thr^3, Val^4 and Glu^5 were selected as the specific sites for N-methyl modification, and a total of eight compounds were prepared by solid peptide synthesis. Their structures are illustrated in Fig. 1.

There were two obstacles in the synthesis of DhHP-6 and its N-methylated derivatives: low coupling efficiency of Dh with the peptide chain due to molecular volume hindrance of Dh and production of low activity by-products, such as a Dh double-coupled peptide chain, since either carboxyl group on the Dh molecule could react with the amide of the peptide. Therefore, we used two strategies to address these problems: (1) low loading resin (0.33 mmol), which reduced the probability of one Dh molecule approaching two peptide chains, and (2) appropriate Dh charge (threefold excess) and reaction time (~60 min). The purity of N-methylated DhHP-6 in the crude peptide preparation was about 50 %, and further processing by RP-HPLC increased the purity of all the DhHP-6 derivatives to above 95 %. The molecular weights of the peptides were also verified by MALDI–TOF-MS analysis (Table 1; Figs. S1–S8).

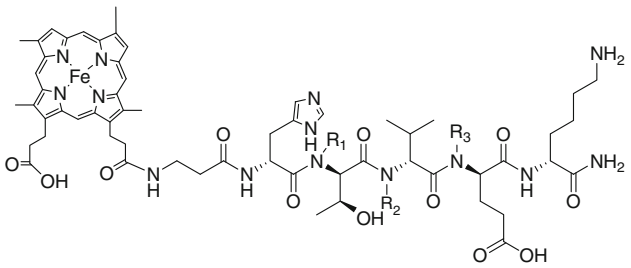

compd	R_1	R_2	R_3
P000	H	H	H
P001	H	H	CH_3
P010	H	CH_3	H
P100	CH_3	H	H
P011	H	CH_3	CH_3
P101	CH_3	H	CH_3
P110	CH_3	CH_3	H
P111	CH_3	CH_3	CH_3

Fig. 1 General structure and nomenclature of DhHP-6 and derivatives. Substituents of the various compounds are indicated. P000 indicates DhHP-6, sic passim

Peroxidase activity

DhHP-6 as a peroxidase mimetic can catalyze electron transfer from reduction substrate to peroxidase. Therefore, the enzymatic potencies of DhHP-6 and its N-methylation derivatives were tested using ascorbic acid and H_2O_2. As shown in Fig. 2, activities of DhHP-6 and the N-methylation derivatives were in the range of 29–34 U/μmol, i.e., 1 mimetic molecule could scavenge about 30 molecules of ascorbic acid and 15 molecules of H_2O_2 per minute, equivalent to the activity of the control enzyme MP-11 of 34 U/μmol. Previous studies have suggested that the imidazole of His^2 coordinating Fe^{3+} on Dh in the axial direction is important for electron transfer to the substrate, as the activity of DhHP-6 was demonstrated to be impaired when the distance between His and Dh was not appropriate and even abolished when His was substituted with Ala (Liu 2003). As modification at the key site of His in DhHP-6 was avoided in this study, the peroxidase activity of the N-methylated derivatives was not significantly influenced.

Determination of in vitro stability

Orally delivered drugs are exposed to abundant metabolic enzymes in the digestive tract, such as pepsin, trypsin, chymotrypsin, elastase, exopeptidase and endopeptidase, before being absorbed into the blood circulation (Woodley 1994; Bernkop-Schnürch and Walker 2001). The low bioavailability of orally administered peptides is mainly the result of rapid degradation in the intestine and insufficient amount of drug passing through the biological barrier. N-methylation has been demonstrated to improve the enzymatic stability of peptides (Linde et al. 2008; Biron et al. 2008). Therefore, we tested the metabolic stability of N-methylation modified DhHP-6 under selected representative physiological conditions by incubating the peptides with serum or intestinal homogenate at 37 °C, and the levels of the remaining native compounds were analyzed by RP-HPLC at several time intervals.

Table 1 Summary of physical and chemical properties of DhHP-6 and derivatives

Compound	HPLC		MS		log $P_{o/w}$
	t_R	%	Theory	Observation	
P000	11.30	98.2	1228.51	1228.46	−3.75
P001	11.33	97.5	1242.53	1242.46	−3.60
P010	11.26	99.7	1242.53	1242.46	−3.64
P100	11.18	99.8	1242.53	1242.47	Nd
P011	11.15	99.2	1256.54	1256.50	−3.41
P101	11.35	95.9	1256.54	1256.51	−3.43
P110	10.85	99.5	1256.54	1256.49	Nd
P111	11.23	98.9	1270.56	1270.49	−3.33

Nd not determined

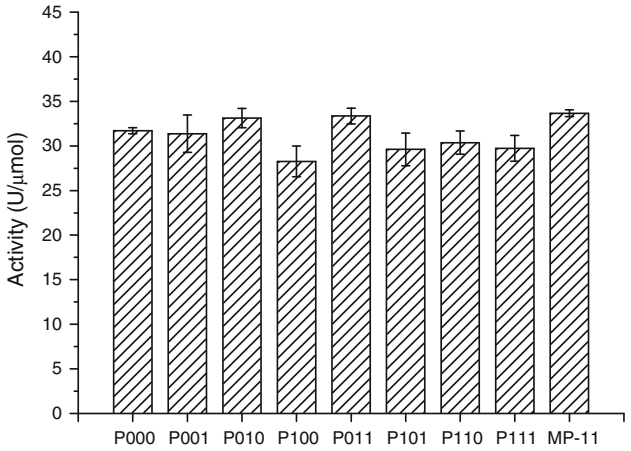

Fig. 2 Hydrogen peroxide scavenging activity of DhHP-6 and derivatives ($n = 3$; mean ± SD)

As shown in Fig. 3, degradation rates of the DhHP-6 derivatives in serum were obviously slower than those in the intestinal homogenate. For example, over 80 % of P000 (i.e., DhHP-6) remained after 24 h in the serum, compared to only about 20 % after 20 min in the intestine. In either case, they were divided into two groups, a stable group (including P111, P101, P011 and P001) and a susceptible group (including P000, P010, P100 and P110). There were subtle differences in the stability in each group. Whereas P111 showed almost no change, P001 was relatively labile in the stable group, and P110 was more stable than P010 in the susceptible group. With respect to the degree of N-methylation, multi-N-methylation modified DhHP-6 resisted protease degradation more effectively than those with mono-N-methylation. For instance, in the stable group, the rank of peptides in order of stability was P111 > P101 > P001, and that of the susceptible group was P110 > P100 > P000. Interestingly, different N-methylation sites of the peptide chain conferred various levels of resistance to protease cleavage. When the amide of Glu, the penultimate residue at the C-terminal end of the peptide, was N-methylated, the enzyme stability of the peptide was significantly enhanced. As shown in Table 2, the half-lives of Pxx1 peptides were obviously improved (e.g., over 8 h for P001, P011, P101 and P111) compared with those for Pxx0 peptides (e.g., between 10 min and 1.2 h for P000, P010, P100 and P110). The Thr residue, adjacent to the His residue of DhHP-6, was another important N-methylation site for protection from enzymatic degradation. For example, the half-life of P100 was threefold greater than that of P010, while the half-life of P101 was about twofold higher than that of P011.

To explore their mechanism of resistance against hydrolysis, the main degradation fragments of DhHP-6 and its derivatives in intestinal homogenate were collected and identified by MALDI–TOF-MS (Table 3 and Figs. S9–S16). Based on the results of MS and MS/MS, a deduced scheme for the degradation of DhHP-6 and its derivatives is shown in Fig. 4. First, DhHP-6 and the derivatives (D6-NH_2) were changed to the corresponding carboxylic acid (D6-OH) by a proteinase or amidase reacting with the C-terminal Lys-amide of the synthesized peptide chain, which was originally cleaved from the rink amide resin. Furthermore, the Lys, Glu, Val and Thr residues were cleaved stepwise from the peptide chain by the carboxypeptidase B or A to form a relatively stable metabolite of Dh-β-AH-OH. An alternate degradation pathway could be cleavage of Dh-peptides by chymotrypsin, which prefers aromatic and hydrophobic amino acid residues, such as Phe, Trp, Met and His, at the amide bond of His–Thr (Wang et al. 2002).

From the molecular structure of DhHP-6, we found that the Dh-blocked N-terminal end of the peptide chain prevents the aminopeptidase or N-terminal dipeptidyl peptidase IV from approaching the amide. For the four remaining sites of potential enzymatic hydrolysis on DhHP-6, His–Thr, Thr–Val, Val–Glu and Glu–Lys, both the connection of β-Ala with Dh through the β-amide and the ring structure resulting from the coordination of His imidazolyl with Fe^{3+} of Dh should endow these sites with resistance against enzymatic attack. Therefore, our results confirmed that carboxypeptidases or endopeptidases likely dominated the fate of the derivatives in the intestinal

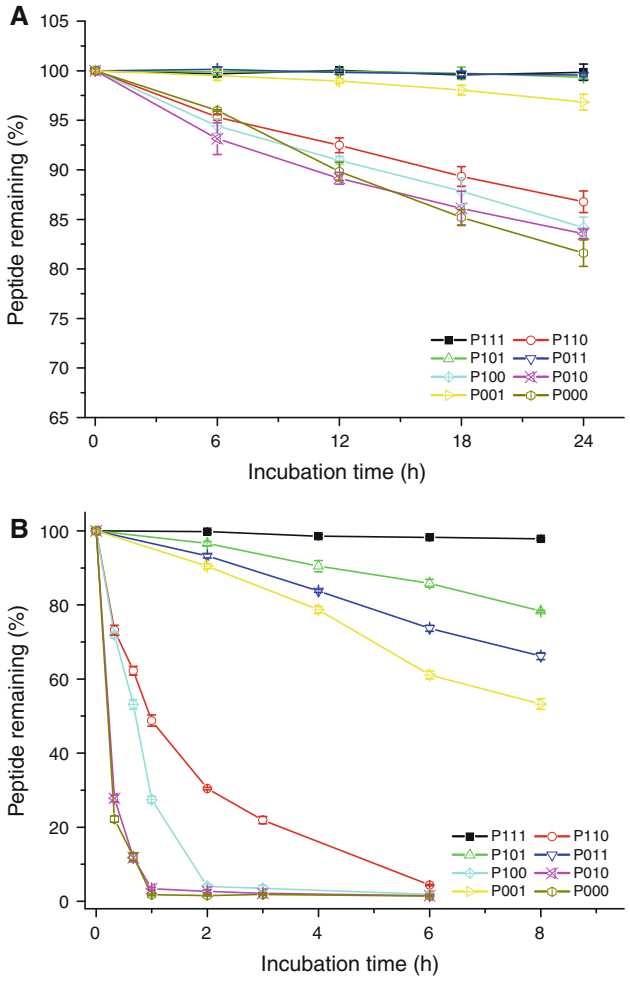

Fig. 3 Degradation of DhHP-6 and derivatives incubated with mouse serum (**a**) and intestinal homogenate (**b**) at 37 °C ($n = 3$; mean ± SD)

Table 2 Half-life of DhHP-6 and derivatives in mouse intestinal homogenate

Compound	Half-life (h)	Fold increase
P000	0.17 ± 0.015	1.0
P001	8.75 ± 0.85	51.5
P010	0.19 ± 0.011	1.1
P100	0.59 ± 0.050	3.5
P011	13.34 ± 0.82	78.5
P101	23.30 ± 2.12	137.1
P110	1.18 ± 0.11	6.9
P111	>24	>141.2

homogenate or serum. The deamination reaction could easily proceed when the N-methylation site was far from the C-terminus, while it was inhibited when the modification was closer to the C-terminal end. N-methylation on the amide bond of Val–Glu effectively conferred resistance to hydrolysis by carboxypeptidase or C-terminal dipeptidyl peptidase, since a compound containing two amides is the optimum substrate structure for those enzymes. For example, D6-OH was the major degradation product of P000, P010, P100 and P110, and it was further cleaved into smaller fragments from P000 and P100. However, among P001, P101 and P011, evidence of deamination was difficult to find, and the low amount of D6-OH was the only cleavage product observed. Moreover, N-methylation of His–Thr hampered endopeptidases, such as chymotrypsin, from recognizing the amide for cleavage. Furthermore, an additional N-methylation on Thr–Val rendered the peptide bond highly resistant to degradation by various enzymes.

The degradation of DhHP-6 derivatives in serum followed a similar pattern (Figs. S17–S24). However, the peptides were not degraded to such a degree as that found in the intestinal homogenate. This can be attributed to the lower concentration or activity of peptidases, especially proteinase or amidase, in the serum. The fact that D6-OH was hydrolyzed fivefold faster than D6-NH_2 indicated that a considerable amount of carboxypeptidase B exists in serum. Because carboxypeptidase can only recognize the carboxyl group (not acid amide) of the peptide, the metabolic rate of DhHP-6 derivatives in serum is limited at the step of D6-NH_2 conversion to D6-OH (Grunwald et al. 2009; Biron et al. 2008). Consequently, the activity of carboxypeptidase B is mainly responsible for maximum effectiveness of the peptides in serum.

A possible explanation for the enhanced protection against enzymatic degradation of the modified peptide is that N-methylation modified amides increase steric hindrance against the approach of proteinases or peptidases to the peptide. N-methylation also prevents the formation of H-bonds between the peptide and the binding site of enzymes, which is essential for the enzyme to recognize its substrate. For example, the conformation of the active center of carboxypeptidase undergoes a significant change in order for hydrolytic activity to occur in the presence of a substrate (Wang et al. 2002). However, activation of enzymes by adjoining in the correct orientation with N-methylated derivatives of DhHP-6 would be relatively more difficult to achieve than with the parent compound, which explains the significantly enhanced stability.

In vitro permeability study

Furthermore, the permeability of DhHP-6 and its N-methylated analogs across the intestinal membrane was investigated using Caco-2 cell monolayers and everted gut sacs, which are general screening models in vitro and ex vivo, respectively, for drug absorption. Comparison of those permeability parameters allows prediction of good candidate compounds for potential oral administration (Burton et al. 1993; Barthe et al. 1999; Artursson and Karlsson 1991).

Table 3 Identification of degradation fragments of DhHP-6 and derivatives in mouse intestinal homogenate by MS analysis

Compd	Sequence	MS (*m/z*)	MS/MS (*m/z*)
P000	Dh-*β*-AHTVEK-NH_2	1228.46	b2(754.25), b3(856.30), b4(955.34), b5(1084.37), y4(475.27), y5(612.35)
	Dh-*β*-AHTVEK-OH	1229.44	b2(755.25), b3(856.29), b4(955.34), b5(1084.37), y4(476.30), y5(613.34)
	Dh-*β*-AHT-OH	873.23	b2(755.21), y2(257.13)
	Dh-*β*-AHTVE-OH	1101.33	b2(755.25), b3(856.30), b4(955.35), y4(485.26)
	Dh-*β*-AH-OH	772.23	b1(617.19), b2(754.26), c1(635.19), y1(155.97)
	Dh-*β*-AHTV-OH	972.29	b2(755.24), b3 + H_2O(874.26), y3(356.20)
P001	Dh-*β*-AHTV(Me)EK-NH_2	1242.50	b2(754.25), b3(855.30), b4(955.36), b5(1098.39)
	Dh-*β*-AHTV(Me)EK-OH	1243.49	b2(755.27), b4(954.38), b5(1098.41), y5(627.38)
	Dh-*β*-AH-OH	772.24	b1(617.19), b2(754.25), c1(635.19), y1(156.09),
P010	Dh-*β*-AHT(Me)VEK-NH_2	1242.46	b2(754.25), b3(856.29), b4(969.33), b5(1098.38), z4(471.32)
	Dh-*β*-AHT(Me)VEK-OH	1243.53	b2(754.27), b3(855.31), b4(968.40), b5(1097.44), y4(490.28)
	Dh-*β*-AHT(Me)VE-OH	1115.42	b2(755.27), b3(855.30), b4(968.38), y4(499.28),
P100	Dh-*β*-AH(Me)TVEK-NH_2	1242.51	b2(754.23), b3(870.31), b4(969.35), b5(1097.39), y2(275.15), z4(471.27)
	Dh-*β*-AH(Me)TVEK-OH	1243.49	b2(754.25), b3(870.31), b4(968.38), y4(490.30), y5(627.38)
	Dh-*β*-AH(Me)TVE-OH	1115.43	b2(755.26), b3(869.32), b4(968.38), y4(499.27)
	Dh-*β*-AH-OH	772.24	b1(617.17), b2(754.25), c1(635.19), y1(156.02)
P011	Dh-*β*-AHT(Me)V(Me)EK-NH_2	1256.52	b3-H_2O(839.35), b5(1112.42), c2(773.24), c4(987.40)
	Dh-*β*-AHT(Me)V(Me)EK-OH	1257.50	b2(754.24), b3(855.26), b4(968.34), b5(1111.37)
P101	Dh-*β*-AH(Me)TV(Me)EK-NH_2	1256.53	b2(754.30), b3(870.34), b4(970.42), b5(1112.37), y4(503.33)
	Dh-*β*-AH(Me)TV(Me)EK-OH	1257.50	b2(754.26), b3(870.30), b4(968.39), b5(1111.44)
	Dh-*β*-AH-OH	772.22	b1(617.18), b2(754.26), c1(635.19), y1(156.07)
P110	Dh-*β*-AH(Me)T(Me)VEK-NH_2	1256.54	b2(754.25), b3(870.30), b4(983.38), b5(1111.41), c2(772.28), z4(485.33)
	Dh-*β*-AH(Me)T(Me)VEK-OH	1257.51	b2(754.27), b3(869.33), b5(1111.44)
			b4-H_2O(965.39), y4-NH_3(486.31)
	Dh-*β*-AH(Me)T(Me)VE-OH	1129.41	b2(754.25), b3(869.31), b4(982.39)
	Dh-*β*-AH-OH	772.23	b1(617.19), b2(754.30), c1(635.21), y1(156.07)
P111	Dh-*β*-AH(Me)T(Me)V(Me)EK-NH_2	1270.55	b2(754.23), b3(870.24), b4(982.36), b5(1125.39), c2(772.24), z4(500.35)
	Dh-*β*-AH-OH	772.22	b1(617.18), b2(754.27), c1(635.19), y1(156.03)

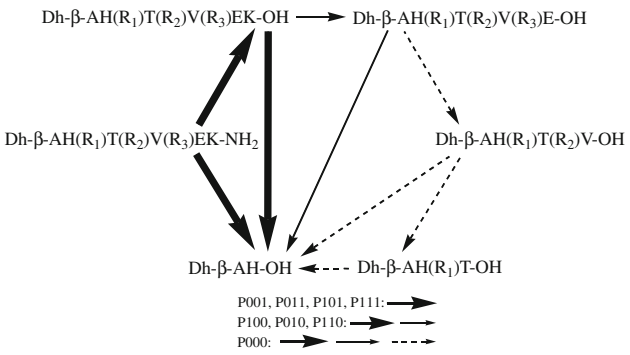

Fig. 4 Putative degradation pathway of DhHP-6 and derivatives in mouse serum and intestinal homogenate. Structures and names of compounds are defined in Fig. 1

In general, a P_{app} less than 10^{-7} cm/s in the Caco-2 cell model indicates that only less than 1 % of the drug can be absorbed in vivo. In our study, all of the DhHP-6 analogs had low permeability (P_{app} ranging from 1.0×10^{-8} to 9.0×10^{-8} cm/s) and thus were intestinally malabsorbed compounds. Compared with P000, the P_{app} of P011, P110, P101 and P010 showed an upward trend, although the permeation differences were not statistically significant. Interestingly, the P_{app} of P111 was 3.4-fold higher than that of P000 (Table 4). Notably, the influx of the tri-N-methylated molecule was greater than those of mono- and di-N-methylated derivatives. These results indicated that not only the N-methylation site, but also the degree of N-methylation influenced the flux of the modified peptides across the Caco-2 cell monolayer, which was consistent with a previous report (Biron et al. 2008).

Although some studies have demonstrated that N-methylation can increase hydrophobicity of peptides, which is one of the most important factors influencing intestinal absorption (Ovadia et al. 2011), in the case of DhHP-6, N-methylation did not significantly increase log $P_{o/w}$ values (Table 1). Most therapeutic proteins/peptides with log $P_{o/w}$ values less than 0 (indicating hydrophilic molecules) are more likely to follow the paracellular pathway, while the transcellular pathway predominates and

Table 4 Apparent permeability coefficients (P_{app}) of DhHP-6 and derivatives across Caco-2 cell monolayers and everted gut sac membranes ($n = 3$; mean ± SD)

Compound	Permeability[a] × 10^8 (cm/s)	Permeability[b] × 10^8 (cm/s)
P000	2.63 ± 0.63	Nd
P001	1.25 ± 0.43	6.90 ± 1.56
P010	4.90 ± 0.96	Nd
P100	1.85 ± 0.85	Nd
P011	3.29 ± 1.43	8.39 ± 1.20
P101	3.35 ± 1.38	9.65 ± 0.97
P110	3.18 ± 0.87	2.38 ± 1.33
P111	8.78 ± 1.55*	11.13 ± 1.05

Nd not determined

* $P < 0.05$ versus P000

[a] Caco-2 cells

[b] Everted gut sac

paracellular effects are less important for those with log $P_{o/w}$ higher than 1 (Mahato et al. 2003). We presume that DhHP-6 and its N-methyl modified analogs are transported through the biological membranes by passive diffusion via paracellular pathways. Therefore, representative peptides P000 and P111 were selected to test the influence of an absorption enhancer, EDTA, on their flux. EDTA is known to increase paracellular permeability through opening tight junctions between cells via Ca^{2+} chelation. As indicated in Fig. 5, EDTA treatment significantly enhanced the flux of P000 and P111 to a degree similar to that of the paracellular marker fluorescein, suggesting that the main mechanism for DhHP-6 derivatives crossing the Caco-2 cell monolayer was through a paracellular pathway (Gan et al. 1993; Artursson and Magnusson 1990), and paracellular absorption enhancers may effectively improve their intestinal absorption.

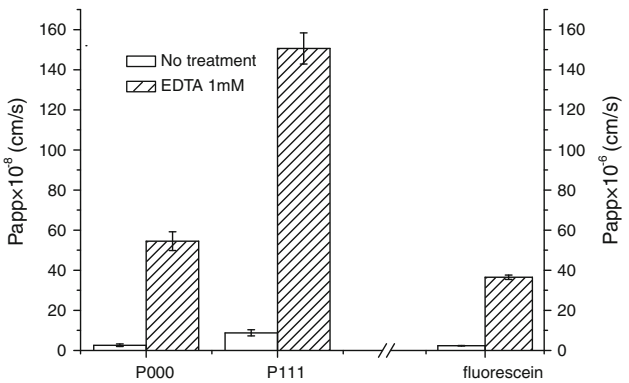

Fig. 5 Effect of absorption enhancer, EDTA, on the permeability of fluorescein, P000 and P111 across Caco-2 cell monolayers ($n = 3$; mean ± SD)

Watson et al. proposed that hydrodynamic volume and conformation are the main factors affecting paracellular transport of molecules. The paracellular pathway contains both restrictive pores serving as a sharp molecular size cutoff and non-restrictive pores which allow the permeation of larger molecules (Hess et al. 2007; Watson et al. 2001). Tri-N-methylation can constrain the diversity of peptide conformations more efficiently than mono- and di-methylation by steric hindrance or can reduce the hydrodynamic volume by inhibiting hydrogen-bonding formation with water, which would help hydrophilic proteins/peptides to diffuse through intercellular junctions (Hess et al. 2007). Accordingly, it is reasonable to presume that P000, P001 or P100 could only pass through non-restrictive pores, while P111 could simultaneously pass through both restrictive and non-restrictive pores, resulting in higher permeability.

In the ex vivo gut sac experiment, P000, P010 and P100 flux through the gut could not be observed, which was probably due to rapid degradation by hydrolytic enzymes on the brush border membrane. However, P001, P011, P101 and P111 were detected with relatively high permeation values due to their excellent stability in the presence of gut proteases. Overall, the P_{app} values of P001, P011, P101 and P111 obtained from the gut sac were greater than those on Caco-2 cell monolayers (Table 4), consistent with the known differences in the tight junction pore sizes between the two models (Lennernäs 1998).

Conclusion

In the present work, we designed and synthesized a series of novel Dh-peptide conjugates through specific multi-site N-methylation modifications of DhHP-6 (i.e., N-Me-Thr, N-Me-Val and N-Me-Glu), which can be used as ROS scavengers for oral administration. All investigated bio-conjugates showed equal ability in scavenging H_2O_2, indicating that their activity was not affected by the N-Me-amino acid substitution. Moreover, N-methylation on specifically selected sites highly reinforced the stability of peptide bonds which are sensitive to hydrolases under physiological conditions. In addition, tri-N-methylation improved the potential of the hydrophilic peptides to pass through bio-membranes to some extent, especially in the presence of an absorption enhancer. However, further structural optimization, such as formation of a rigidity ring, conjugation with an absorption enhancer or a cell-penetrating peptide, is needed to improve the transcellular permeability of these promising bio-conjugates for oral administration.

Acknowledgments This work was supported by the National Natural Science Foundation of China (No. 30901863, 20872048) and China Postdoctoral Science Foundation (No. 20110491321). We gratefully acknowledge Hui Cai and Xu Yang (Changchun BCHT Co. Ltd.) for their assistance with peptide synthesis.

Conflict of interest The authors declare no conflict of interest.

References

Artursson P, Karlsson J (1991) Correlation between oral drug absorption in humans and apparent drug permeability coefficients in human intestinal epithelial (Caco-2) cells. Biochem Biophys Res Commun 175:880–885

Artursson P, Magnusson C (1990) Epithelial transport of drugs in cell culture. II: Effect of extracellular calcium concentration on the paracellular transport of drugs of different lipophilicities across monolayers of intestinal epithelial (Caco-2) cells. J Pharm Sci 79:595–600

Barthe L, Woodley JF, Kenworthy S, Houin G (1998) An improved everted gut sac as a simple and accurate technique to measure paracellular transport across the small intestine. Eur J Drug Metab Pharmacokinet 23:313–323

Barthe L, Woodley JF, Houin G (1999) Gastrointestinal absorption of drugs: methods and studies. Fundam Clin Pharmacol 13:154–168

Berlett BS, Stadtman ER (1997) Protein oxidation in aging, disease, and oxidative stress. J Biol Chem 272:20313–20316

Bernkop-Schnürch A, Walker G (2001) Multifunctional matrices for oral peptide delivery. Crit Rev Ther Drug Carrier Syst 18:459–501

Biron E, Chatterjee J, Ovadia O, Langenegger D, Brueggen J, Hoyer D, Schmid HA, Jelinek R, Gilon C, Hoffman A, Kessler H (2008) Improving oral bioavailability of peptides by multiple N-methylation: somatostatin analogues. Angew Chem Int Ed Engl 47:2595–2599

Burton PS, Conradi RA, Hilgers AR, Ho NF (1993) Evidence for a polarized efflux system for peptides in the apical membrane of Caco-2 cells. Biochem Biophys Res Commun 190:760–766

Chatterjee PK, Patel NS, Kvale EO, Brown PA, Stewart KN, Mota-Filipe H, Sharpe MA, Di Paola R, Cuzzocrea S, Thiemermann C (2004) EUK-134 reduces renal dysfunction and injury caused by oxidative and nitrosative stress of the kidney. Am J Nephrol 24:165–177

Chatterjee J, Gilon C, Hoffman A, Kessler H (2008) N-methylation of peptides: a new perspective in medicinal chemistry. Acc Chem Res 41:1331–1342

Day BJ (2004) Catalytic antioxidants: a radical approach to new therapeutics. Drug Discov Today 9:557–566

Gan LS, Niederer T, Eads C, Thakker D (1993) Evidence for predominantly paracellular transport of thyrotropin-releasing hormone across Caco-2 cell monolayers. Biochem Biophys Res Commun 197:771–777

Gao JN, Hugger ED, Beck-Westermeyer MS, Borchardt RT (2001) Estimating intestinal mucosal permeation of compounds using Caco-2 cell monolayers. Curr Protoc Pharmacol Chapter 7:Unit 7.2

Gentilucci L, De MR, Cerisoli L (2010) Chemical modifications designed to improve peptide stability: incorporation of non-natural amino acids, pseudo-peptide bonds, and cyclization. Curr Pharm Des 16:3185–3203

Grunwald J, Rejtar T, Sawant R, Wang Z, Torchilin VP (2009) TAT peptide and its conjugates: proteolytic stability. Bioconjug Chem 20:1531–1537

Guan SW, Li PF, Luo J, Li YY, Huang L, Wang G, Zhu LM, Fan HK, Li W, Wang LP (2010) A deuterohemin peptide extends lifespan and increases stress resistance in *Caenorhabditis elegans*. Free Radic Res 44:813–820

Hamman JH, Enslin GM, Kotzé AF (2005) Oral delivery of peptide drugs: barriers and developments. BioDrugs 19:165–177

Han HK, Stewart BH, Doherty AM, Cody WL, Amidon GL (1998) In vitro stability and intestinal absorption characteristics of hexapeptide endothelin receptor antagonists. Life Sci 63:1599–1609

Hess S, Ovadia O, Shalev DE, Senderovich H, Qadri B, Yehezkel T, Salitra Y, Sheynis T, Jelinek R, Gilon C, Hoffman A (2007) Effect of structural and conformation modifications, including backbone cyclization, of hydrophilic hexapeptides on their intestinal permeability and enzymatic stability. J Med Chem 50:6201–6211

Lee HJ (2002) Protein drug oral delivery: the recent progress. Arch Pharm Res 25:572–584

Lennernäs H (1998) Human intestinal permeability. J Pharm Sci 87:403–410

Linde Y, Ovadia O, Safrai E, Xiang Z, Portillo FP, Shalev DE, Haskell-Luevano C, Hoffman A, Gilon C (2008) Structure–activity relationship and metabolic stability studies of backbone cyclization and N-methylation of melanocortin peptides. Biopolymers 90:671–682

Lister-James J, Dean RT, Pearson DA, Wilson DM (2001) Novel somatostatin analogs. WO 01/44177 A2

Liu, YL (2003) Peptide mimics of peroxidase with anti-cataract activity. Dissertation, University of Jilin, pp 65–70

Liu YL, Guo LL, Roger R, Luo GM, Li W (2001) The method improvement of synthesis and purification of deuterohemin. Acta Sci Nat Univ Jilin, 91–92

Mahato RI, Narang AS, Thoma L, Miller DD (2003) Emerging trends in oral delivery of peptide and protein drugs. Crit Rev Ther Drug Carrier Syst 20:153–214

Mandelman D, Schwarz FP, Li H, Poulos TL (1998) The role of quaternary interactions on the stability and activity of ascorbate peroxidase. Protein Sci 7:2089–2098

Masini E, Cuzzocrea S, Mazzon E, Marzocca C, Mannaioni PF, Salvemini D (2002) Protective effects of M40403, a selective superoxide dismutase mimetic, in myocardial ischaemia and reperfusion injury in vivo. Br J Pharmacol 136:905–917

Nakabeppu Y, Tsuchimoto D, Yamaguchi H, Sakumi K (2007) Oxidative damage in nucleic acids and Parkinson's disease. J Neurosci Res 85:919–934

Nestor JJ Jr (2009) The medicinal chemistry of peptides. Curr Med Chem 16:4399–4418

Ovadia O, Greenberg S, Chatterjee J, Laufer B, Opperer F, Kessler H, Gilon C, Hoffman A (2011) The effect of multiple N-methylation on intestinal permeability of cyclic hexapeptides. Mol Pharm 8:479–487

Reed TT (2011) Lipid peroxidation and neurodegenerative disease. Free Radic Biol Med 51:1302–1319

Rice-Evans CA, Diplock AT (1993) Current status of antioxidant therapy. Free Radic Biol Med 15:77–96

Smith KR, Uyeminami DL, Kodavanti UP, Crapo JD, Chang L, Pinkerton KE (2002) Inhibition of tobacco smoke-induced lung inflammation by a catalytic antioxidant. Free Radic Biol Med 33:1106–1114

Takács-Novák K, Avdeef A, Box KJ, Podányi B, Szász G (1994) Determination of protonation macro- and microconstants and octanol/water partition coefficient of the antiinflammatory drug niflumic acid. J Pharm Biomed Anal 12:1369–1377

Wang JY, Zhu SG, Xu CF (2002) Biochemistry, 3rd edn. Higher education press, Beijing, pp 174, 402–405

Wang LP, Liu YL, Yang H, Li W (2004) Synthesis and anti-cataract activity of a novel peroxidase mimetics. Chem J Chin Univ 25:2171–2173

Watson CJ, Rowland M, Warhurs G (2001) Functional modeling of tight junctions in intestinal cell monolayers using polyethylene glycol oligomers. Am J Physiol Cell Physiol 281:C388–C397

Woodley JF (1994) Enzymatic barriers for GI peptide and protein delivery. Crit Rev Ther Drug Carrier Syst 11:61–95